Human Molecular Genetics, 2013, Vol. 22, No. 23 **4706–4719**
doi:10.1093/hmg/ddt319
Advance Access published on July 4, 2013

The ALS disease-associated mutant TDP-43 impairs mitochondrial dynamics and function in motor neurons

Wenzhang Wang[1,†], Li Li[1,3,†], Wen-Lang Lin[2], Dennis W. Dickson[2], Leonard Petrucelli[2], Teng Zhang[3] and Xinglong Wang[1,*]

[1]Department of Pathology, Case Western Reserve University, Cleveland, OH 44106, USA, [2]Department of Neuroscience, Mayo Clinic, Jacksonville, FL 32224, USA and [3]Yueyang Hospital and Clinical Research Institute of Integrative Medicine, Shanghai University of Traditional Chinese Medicine, Shanghai 200437, China

Received May 20, 2013; Revised June 25, 2013; Accepted July 1, 2013

Mutations in TDP-43 lead to familial ALS. Expanding evidence suggests that impaired mitochondrial dynamics likely contribute to the selective degeneration of motor neurons in SOD1-associated ALS. In this study, we investigated whether and how TDP-43 mutations might impact mitochondrial dynamics and function. We demonstrated that overexpression of wild-type TDP-43 resulted in reduced mitochondrial length and density in neurites of primary motor neurons, features further exacerbated by ALS-associated TDP-43 mutants Q331K and M337V. In contrast, suppression of TDP-43 resulted in significantly increased mitochondrial length and density in neurites, suggesting a specific role of TDP-43 in regulating mitochondrial dynamics. Surprisingly, both TDP-43 overexpression and suppression impaired mitochondrial movement. We further showed that abnormal localization of TDP-43 in cytoplasm induced substantial and widespread abnormal mitochondrial dynamics. TDP-43 co-localized with mitochondria in motor neurons and their colocalization was enhanced by ALS associated mutant. Importantly, co-expression of mitochondrial fusion protein mitofusin 2 (Mfn2) could abolish TDP-43 induced mitochondrial dynamics abnormalities and mitochondrial dysfunction. Taken together, these data suggest that mutant TDP-43 impairs mitochondrial dynamics through enhanced localization on mitochondria, which causes mitochondrial dysfunction. Therefore, abnormal mitochondrial dynamics is likely a common feature of ALS which could be potential new therapeutic targets to treat ALS.

INTRODUCTION

Amyotrophic lateral sclerosis (ALS) is the most common of the five motor neuron diseases characterized by progressive neurodegeneration of motor neurons in the brain stem and spinal cord. The vast majority of ALS cases, referred to as sporadic ALS, are not genetically transmitted and their causes remain enigmatic. Less than 10% of ALS cases are familial, involving mutations in several genes such as C9orf72, SOD1, TARDBP, FUS and ANG. Although TARDBP gene mutations account for about 4% of familial ALS, the protein encoded by TARDBP, i.e. TAR DNA-binding protein 43 (TDP-43), was identified as a major component of the histopathological hallmark, i.e. neuronal ubiquitinated inclusions, of degenerating neurons in most sporadic and familial ALS cases (1). Indeed, the presence of TDP-43 was also reported as the primary histopathological feature of frontotemporal lobar degeneration (FTLD) (2) and as secondary histopathological feature of other neurodegenerative diseases such as Alzheimer's disease (AD) (3), Parkinson's disease (PD) (4) and Huntington's disease (HD) (5).

TDP-43 is a highly conserved and ubiquitously expressed DNA/RNA binding protein containing two RNA recognition motifs and a C-terminal glycine-rich domain. All ALS-associated mutations in TDP-43 cluster in the C-terminal glycine-rich domain that is thought to be important for interaction with heterogeneous

*To whom correspondence should be addressed at: Department of Pathology, Case Western Reserve University, 2103 Cornell Road, Cleveland, OH 44106, USA. Tel: +1 2163682957; Fax: +1 2163688964; Email: xinglong.wang@case.edu
†Both authors contributed equally to this work.

nuclear ribonucleoproteins to mediate transcription, pre-mRNA splicing, mRNA processing and microRNA biogenesis (6–8). TDP-43 is mainly localized in the nucleus under normal conditions, whereas it is depleted from the nucleus and accumulates in cytoplasmic ubiquitinated inclusions in affected motor neurons from ALS patients. Until now, no consensus has emerged as to whether TDP-43 dysfunction caused by nuclear depletion, cytoplasmic accumulation of insoluble TDP-43 or both of them contributes to the onset and progression of ALS.

Abundant evidence has revealed a prominent role for mitochondrial dysfunction in the pathogenesis of ALS (9), although the underlying mechanism is still not clear. Mitochondria are highly dynamic organelles that undergo continual fission/fusion events which serve crucial physiological function (10). Abnormal mitochondrial dynamics can cause mitochondrial dysfunction because of the defective assembly of the ETC complexes (11). Interestingly, the copper–zinc superoxide dismutase (SOD1) encoded by the first discovered and the most common gene associated with familial ALS, localizes to, and directly participates in the regulation of mitochondrial dynamics including fission, fusion, movement and bioenergetics, suggesting impaired mitochondrial dynamics could be the potential mechanism leading to mitochondrial and neuronal dysfunction/degeneration critical to ALS pathogenesis (12). Although expanding evidence suggest a central role of TDP-43 proteinopathy in the pathogenesis of ALS (1), even as increasing numbers of TDP-43 targeted RNAs are identified, the pathogenic mechanisms underlying TDP-43 mediated neurodegeneration remain unknown. Interestingly, recent studies in mice models revealed that overexpression of either wild-type TDP-43 or ALS-associated mutant TDP-43 M337V caused abnormal cytoplasmic mitochondrial aggregates in the cell bodies of motor neurons (13,14), indicating a potential role of TDP-43 in regulating mitochondrial dynamics. Therefore, in this study, we investigated the effects of TDP-43 overexpression or knockdown on mitochondrial dynamics including morphology, distribution and movement and its contribution to TDP-43-induced mitochondrial dysfunction in motor neurons.

RESULTS

TDP-43 regulates mitochondrial morphology in motor neurons

We first investigated the effect of TDP-43 on mitochondria dynamics in primary motor neurons isolated from E13.5 mouse embryos. Motor neurons (DIV = 7) were transiently co-transfected with flag-tagged wild-type (WT) or ALS-associated mutant TDP-43 (Q331K and M337V) and mito-DsRed2 to label mitochondria. Two days after transfection, neurons were fixed, stained for flag, neuronal marker β-III tubulin or motor neuron marker Islet-1 and imaged by laser confocal microscopy. Positively co-transfected cells were selected by the presence of both flag staining and DsRed2 fluorescence (Supplementary Material, Fig. S1A). In neurons expressing WT or mutant TDP-43, the intensity of mito-DsRed2 and flag tagged TDP-43 demonstrated relative large standard deviation but with similar mean values (Supplementary Material, Fig. S1B), suggesting the similar expression levels of WT and mutant TDP-43. Mitochondria in neurons, especially those in cell bodies of neurons, are usually not on the same focal plane and measurement of mitochondrial morphology based on two dimension image from single focal plane could be misleading. To more accurately measure mitochondria morphology and coverage in different compartments of neurons (i.e. axon, dendrite and soma), we acquired series of stacks of images along the z-axis of the neurons and 3D reconstruction of mito-DsRed2 was obtained. On average, dendrites demonstrated longer mitochondria with denser coverage than axons (Fig. 1A). Most control neurons or empty vector-transfected neurons (>90%) demonstrated evenly distributed heterogeneous but predominantly tubular mitochondrial morphology in axon, dendrites and cell bodies (Fig. 1A–D). However, there was a trend towards decreased mitochondrial length in the dendrites of motor neurons expressing WT TDP-43, which became significant in the dendrites of neurons expressing TDP-43 mutants (Fig. 1B). Mitochondrial density/coverage in dendrites as indicated by neurite mitochondria index (total mitochondrial length/neurite length) was also significantly reduced in motor neurons expressing either WT or mutant TDP-43 (Fig. 1C). Similarly, in the soma, the average mitochondrial length was significantly decreased from 2.1 ± 0.15 μm in control neurons to 1.5 ± 0.11, 1.5 ± 0.15 and 1.2 ± 0.12 μm in WT, Q331K and M337V TDP-43 expressing neurons, respectively (Fig. 1D). Interestingly, in the axon, no difference in mitochondrial length or density/coverage was noted between control and WT or mutant TDP-43 expressing neurons (Supplementary Material, Fig. S1C and D).

To confirm our primary findings *in vivo*, we next studied the effect of WT and mutant TDP-43 on mitochondria in motor neurons in the anterior horn of 1-month old non-transgenic mice (NTG) and transgenic mice overexpressing WT or M337V mutant TDP-43 under the control of the mouse PRNP (prion protein) gene promoter (i.e. WT and M337V mice) (13,14). Consistent with the confocal microscopy results, electron microscopic analysis revealed that significantly shorter and smaller mitochondria dominate the cell bodies of anterior horn motor neurons in both WT and M337V transgenic mice (Fig. 2). Damaged mitochondria as evidenced by the loss of internal cristae structure were rare in the neurons of non-Tg mouse but dominant in the neurons of either WT or M337V mouse.

We then tested whether TDP-43 suppression would induce an effect on mitochondria dynamics opposite to TDP-43 overexpression. Mouse motor neurons (DIV = 7) were transfected with microRNA expression construct miR-TDP-43b reported before that could express both DsRed2 to label cells and pre-miRNA to target mouse or rat TDP-43 (15). Mito-AcGFP was co-transfected to label mitochondria (Supplementary Material, Figs S1A and S3A). Compared with control neurons or neurons expressing miRNA with scrambled sequence (scrambled RNAi), TDP-43 knockdown significantly increased the average mitochondrial length in dendrites and cell bodies but had no effects on mitochondria in axons (Fig. 3B). Mitochondrial density in dendrites was also significantly increased by TDP-43 knockdown (Fig. 3C).

TDP-43 tips the balance of mitochondrial fission and fusion

Mitochondria morphology is tightly regulated by the balance between fission and fusion processes. We investigated the

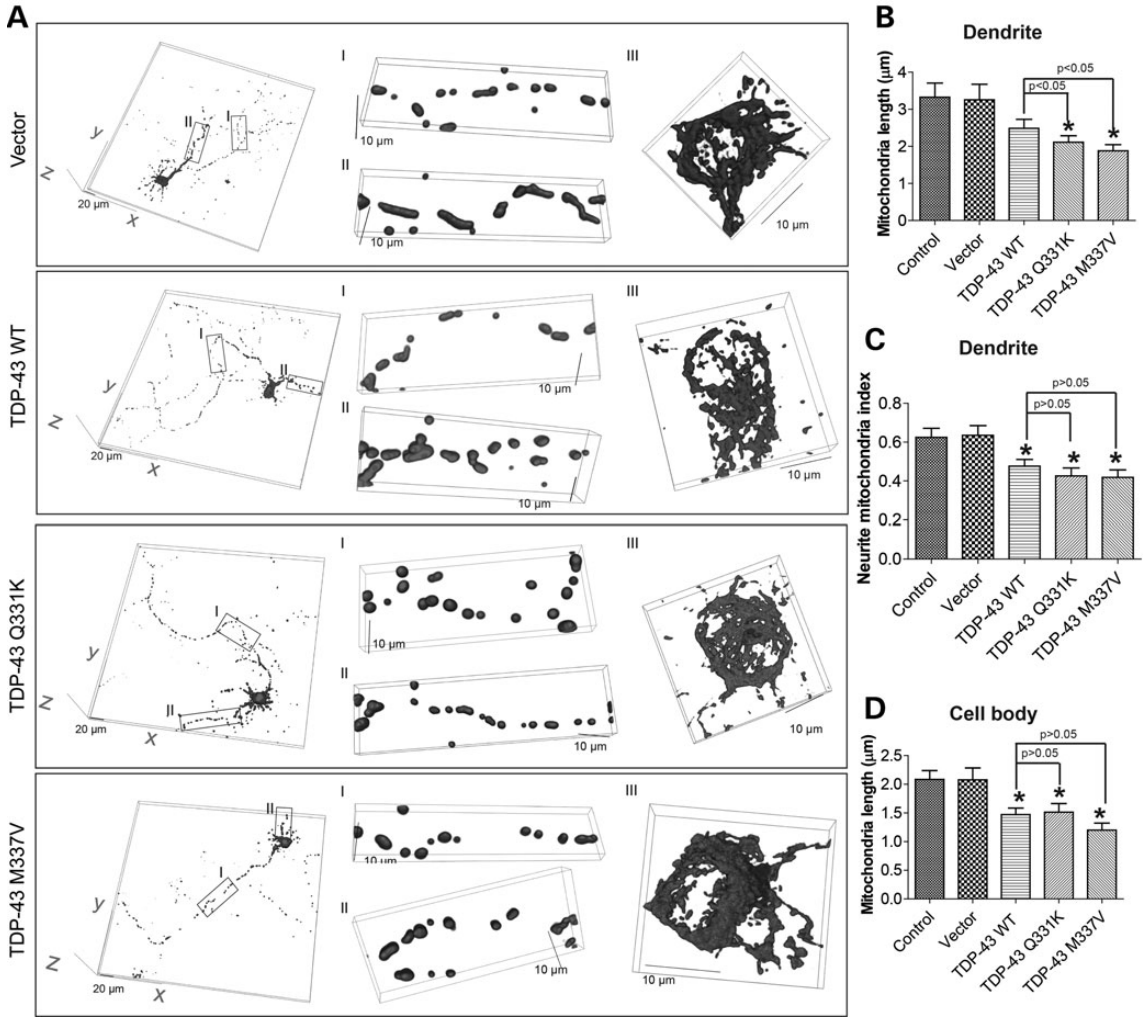

Figure 1. Effect of TDP-43 overexpression on mitochondrial morphology. (**A**) Representative 3-dimensional (3D) pictures of mitochondria in primary rat motor neurons at day *in vitro* 9 (DIV9) co-transfected with constructs encoding flag tagged TDP-43 and mito-DsRed2 at DIV7. Vector: neurons expressing empty vector; TDP-43 WT: neurons expressing wild-type TDP-43; TDP-43 Q331K: neurons expressing mutant TDP-43 Q331K; TDP-43 M337V: neurons expressing mutant TDP-43 M337V. Left panels: large field of view of mitochondria in motor neurons; Middle panels: enlargement showing mitochondria in axons (enlargement I) and dendrites (enlargement II). Right panels: enlargement showing mitochondria in cell bodies (enlargement III). (**B** and **C**) Quantification of mitochondria length (B) and density (i.e. neurite mitochondria index = total mitochondrial length/neurite length) (C) in dendrites. (**D**) Quantification of mitochondria length in cell bodies. Control: control neurons expressing mito-DsRed2 only. At least 20 neurons were analyzed in each experiment and experiments were repeated three times. Data are means ± s.e.m. Statistics: one-way analysis of variance (ANOVA) followed by Tukey's multiple comparison test. $^*P < 0.05$, compared with control neuron.

effects of TDP-43 expression on mitochondrial fission and fusion events by live imaging. Motor neurons (DIV = 7) were transiently co-transfected with blue fluorescent protein (BFP)-tagged WT or mutant TDP-43 (TDP-43-BFP) and mito-DsRed2, and imaged 2 days after transfection in a well-equipped live imaging station with controlled CO_2, humidity and temperature. The positively transfected cells were identified by the presence of bright blue signal (Supplementary Material, Fig. S2). The relatively high density of mitochondria in cell bodies makes it difficult to measure individual mitochondria fission and fusion processes there. Therefore, we only focused on mitochondria in neurites including axons and dendrites. In control neurons, mitochondria in both axons and dendrites underwent rapid and balanced fission and fusion events and the ratio of fission events over fission-plus-fusion events was around 50% (Fig. 4A and B). In contrast, the ratio of fission events over fission-plus-fusion events was significantly increased in the dendrites but not in the axons of neurons expressing mutant TDP-43, suggesting that fission and fusion balance was tipped towards more fission, which was consistent with observed morphological change (Fig. 1).

Similarly, we also measured mitochondrial fission and fusion events in motor neurons with suppressed TDP-43 expression by DsRed-tagged miR-TDP-43b. As expected, TDP-43 knockdown significantly decreased the ratio of fission events over fission-plus-fusion events in dendrites but not in axons (Fig. 4C), consistent with the observed elongated phenotype (Fig. 3).

TDP-43 impairs mitochondrial transport

Axonal mitochondrial transport was reported to be impaired in ALS neurons (16). We next investigated the effects of TDP-43

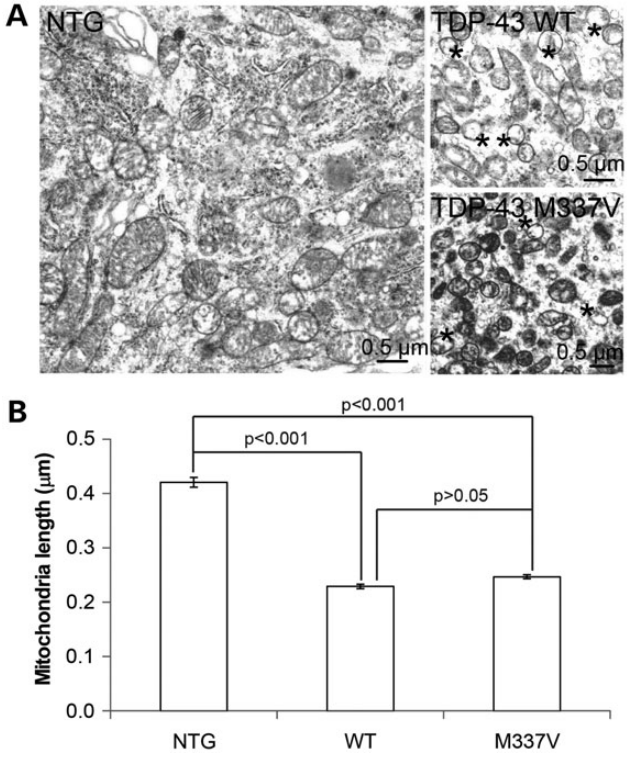

Figure 2. Electron microscopy analysis of mitochondrial morphology in Tg mice. (**A**) Representative EM micrographs of mitochondria in spinal motor neurons of transgenic mice overexpressing wild-type TDP-43 (WT) or mutant TDP-43 M337V (M337V) or age-matched non-transgenic wild-type mouse (NTG). In both TDO-43 WT and M337V mice, many mitochondria demonstrate damaged internal cristae, marked by asterisk, a feature not evident in NTG mice. (**B**) Quantitative analysis of mitochondrial length in motor neurons based on EM micrographs. 653, 274, 726 mitochondria were analyzed for NTG, WT, M337V neurons, respectively. Data are means ± s.e.m. Statistics: one-way analysis of variance (ANOVA) followed by Tukey's multiple comparison test.

expression on mitochondrial transport by live imaging of neurons expressing TDP-43-BFP and mito-DsRed2. Because of high mitochondria density in the proximal segment of axon and dendrite, we focused on mitochondria in the middle segment of axon (100 μm in length beginning 300 μm from the cell body of neurons) and in the distal segment of dendrites (around 50 μm in length beginning from the tip of dendrite). Movement of mitochondria in the axon included both anterograde and retrograde movement, and mitochondria with velocity <0.05 μm/s were classified as stationary. As microtubules exhibit mixed polarity in dendrites especially in proximal regions and mitochondria could be moved in either the anterograde or the retrograde direction (17), only the percentage of stationary mitochondria was quantified and did not differentiate anterograde or retrograde movement in the dendrites. In control neurons, more than 40% of mitochondria in axon and more than 25% of mitochondria in dendrites were mobile and axonal mitochondria demonstrated balanced anterograde and retrograde moving during recording (30 min) (Fig. 5A–C). In contrast, there was significant increase of the percentage of stationary mitochondria in the axons and there was a decreased percentage mitochondria moving in either the anterograde or retrograde direction in neurons expressing WT TDP-43. Similarly, there was a significant decrease in the percentage of mobile mitochondria in dendrites in these neurons. Both ALS-associated mutants caused significant increase of the proportion of stationary mitochondria in both axon and dendrites. Compared with neurons overexpressing WT TDP-43, there was further reduction in the percentage of mitochondria moving in either anterograde or retrograde direction in axons, and a trend of further decrease in the percentage of mobile mitochondria in dendrites in neurons overexpressing mutant TDP-43. In addition, quantification analysis revealed that the average velocity of mobile mitochondria was significantly decreased by TDP-43 overexpression in both axons and dendrites (Fig. 5D and E). We also measured the effect of TDP-43 suppression on mitochondrial transportation. Unexpectedly, TDP-43 RNAi also significantly decreased moving mitochondria in both axons and dendrites similar to TDP-43 overexpression (Fig. 6).

Cytoplasmic TDP-43 causes more severe abnormality in mitochondrial dynamics

In affected ALS neurons, TDP-43 redistributes to the cytoplasm and forms aggregates. Consistent with previous studies (18), most cultured motor neurons with exogenous expression of WT TDP-43 showed mainly nuclear localization of TDP-43 (Supplementary Material, Figs S1A and S7A), whereas $<10\%$ neurons exhibited abnormal cytoplasmic accumulation and nuclear depletion of TDP-43 (Fig. 7A and Supplementary Material, Fig. S3A), which was defined as neurons with abnormal TDP-43 localization. The percentage of neurons demonstrating abnormal TDP-43 localization was significantly increased to more than 20% by familial ALS-associated mutations (Fig. 7B). The average levels of TDP-43 immunofluorescent intensity were similar in WT and mutant TDP-43 expressing neurons with or without abnormal TDP-43 localization (Supplementary Material, Fig. S3B), suggesting the increased cytoplasmic TDP-43 localization in mutant TDP-43 expressing neurons was not due to different expression levels of TDP-43 protein. In those neurons with abnormal TDP-43 localization, the cytoplasmic TDP-43 was present abundantly in both cell body and neurites including axons and dendrites, and no difference in staining pattern was noted between WT or mutant TDP-43 expressing neurons. Interestingly, compared with neurons with normal nuclear localization of TDP-43, neurons with abnormal TDP-43 localization (i.e. cytoplasmic accumulation and nuclear depletion) demonstrated significant mitochondrial fragmentation in the axon (Fig. 7C and Supplementary Material, Fig. S3). It is of importance to note that mitochondrial length in this subgroup of neurons in both WT or mutant TDP-43 expressing neurons was also significantly shorter than in control or vector control neurons despite the fact that there was no difference in mitochondrial length in the overall population of neurons between these groups (Supplementary Material, Fig. S1B and C). Neurons with abnormal TDP-43 localization also demonstrated more significant mitochondrial fragmentation in the dendrites and cell bodies (Fig. 7D and E). Interestingly, in those neurons with abnormal TDP-43 localization, no further decrease of mitochondria length by mutant TDP-43 was observed. The mitochondria density/coverage in both axons and dendrites was also found to be severely reduced in all neurons with abnormal TDP-43 distribution (Fig. 7F and G). Abnormal mitochondrial distribution

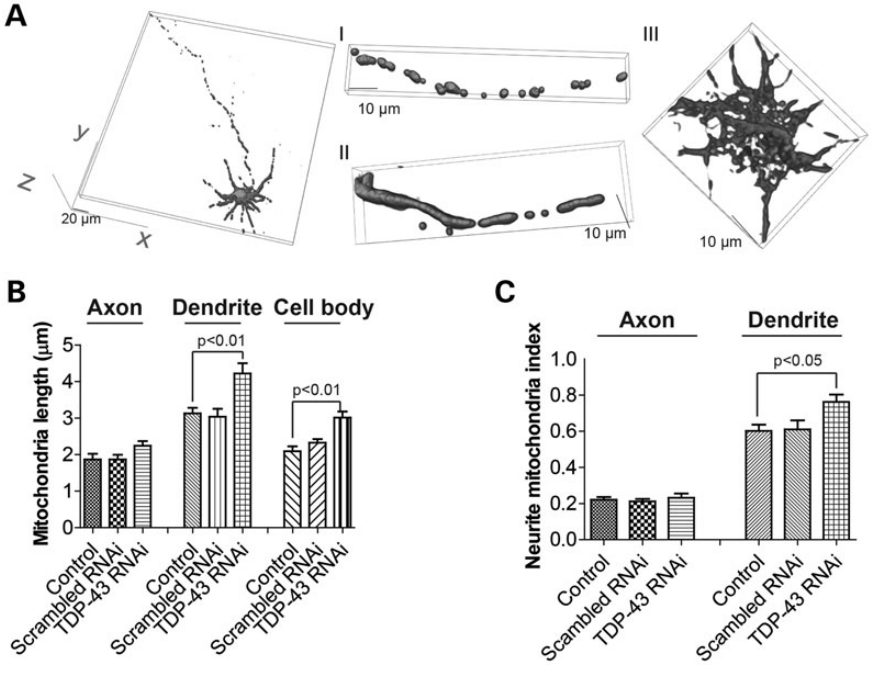

Figure 3. Effect of TDP-43 knockdown on mitochondrial morphology. (**A**) Representative 3D pictures of mitochondria in primary rat motor neurons at DIV9 co-transfected with construct knocking down TDP-43 and construct encoding mito-AcGFP at DIV7. Scrambled RNAi: neurons expressing scramble RNAi; TDP-43 RNAi: neurons expressing pre-miRNA to target TDP-43. Left panel: large field of view of mitochondria in motor neurons; Middle panel: enlargement showing mitochondria in axons (enlargement I) and dendrites (enlargement II). Right panel: enlargement showing mitochondria in cell bodies (enlargement III). (**B** and **C**) Quantification of mitochondria length (B) and density (i.e. neurite mitochondria index = total mitochondrial length/neurite length) (C) in axons, dendrites and/or cell bodies. Control: control neurons expressing mito-AcGFP only. At least 20 neurons were analyzed in each experiment and experiments were repeated three times. Data are means ± s.e.m. Statistics: one-way analysis of variance (ANOVA) followed by Tukey's multiple comparison test.

also occurs in the soma since mitochondria were aggregated around the peri-nuclear area in this subset of neurons (13,14). Further analysis of mitochondrial fission/fusion events revealed that both fission and fusion were severely impaired in neurons with abnormal TDP-43 localization. In fact, fusion events were rarely seen (Fig. 7H). Analysis for mitochondrial movement demonstrated that only few mitochondria were moving in axons and dendrites, and the average velocity of mitochondria was markedly decreased (Supplementary Material, Fig. S4).

TDP-43 co-localizes with mitochondria in the cytoplasm

Recently, it was shown that TDP-43 can localize in the dendrites and axons in motor neurons under normal conditions (18). In our experiments, we noticed that, in motor neurons with cytoplasmic TDP-43 localization (Fig. 7A), flag-tagged TDP-43 co-localized with mitochondria. To exclude the possibility that this colocalization was artificial due to protein or mitochondrial aggregation, we directly investigated the association of TDP-43 and mitochondria in motor neurons with normal localization (i.e. mainly nuclear). Indeed, we found that even in these neurons, TDP-43 also co-localizes with mitochondria in both dendrites and axons (Fig. 8A). Quantification revealed that compared with WT TDP-43, both ALS-associated mutants had significantly enhanced mitochondrial localization of TDP-43 both in axons and dendrites (Fig. 8B and C). We further performed immunoblot analysis of TDP-43 in the mitochondrial fraction prepared from normal NSC-34 motor-like neuronal cells and found that TDP-43 is indeed present in mitochondria under physiological conditions (Fig. 8D).

Mfn2 overexpression prevents TDP-43-induced mitochondrial dynamic abnormalities

Previous studies showed that overexpression of mitochondria fusion protein Mfn2 in neurons could not only increase mitochondrial length but also enhance mitochondrial movement. As our data found both mitochondrial morphology and movement were impaired by WT, and especially mutant TDP-43 overexpression, we next tested whether Mfn2 overexpression could alleviate TDP-43 induced mitochondrial dynamic abnormalities in motor neurons. We co-transfected motor neurons (DIV = 7) with BFP tagged TDP-43 M337V, GFP tagged Mfn2 and mito-DsRed2 (Supplementary Material, Fig. S5A). Two days after transfection, neurons were either fixed or directly imaged. Compared with neurons expressing TDP-43 M337V only, neurons expressing both TDP-43 M337V and Mfn2 had similar percentage of neurons with abnormal TDP-43 localization (Supplementary Material, Fig. S5B). Consistent with previous study (19), Mfn2 overexpression alone caused significant increase of mitochondrial length in axons and cell bodies (Supplementary Material, Figs S5C, D and S9A, B and D) and a trend towards increased mitochondrial length in dendrites (Fig. 9C). Neurite mitochondrial density was also increased significantly by Mfn2 overexpression in axons. Compared with data shown in Figure 1, mitochondrial length and density in axons, dendrites

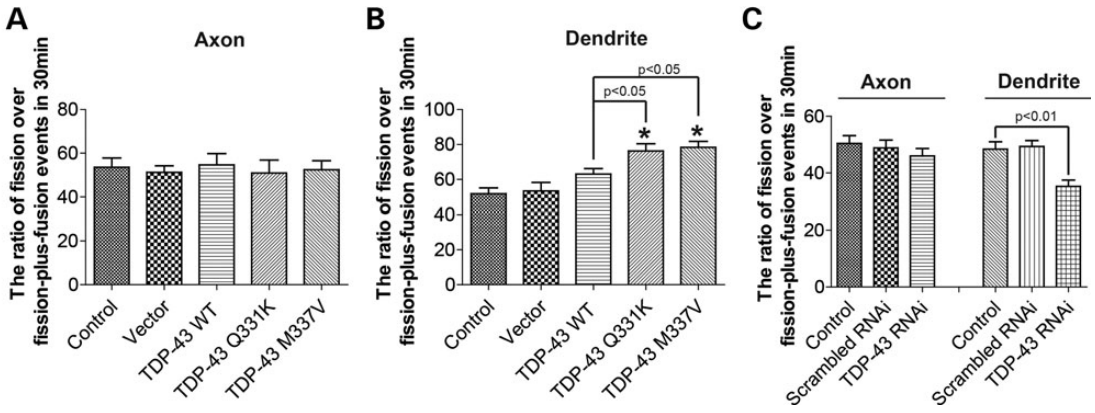

Figure 4. Effect of TDP-43 overexpression or knockdown on mitochondrial fission and fusion dynamics in live cultured motor neurons. Primary rat motor neurons were co-transfected with constructs encoding BFP tagged TDP-43/DsRed tagged miR-TDP-43b and mito-DsRed2/mito-AcGFP at DIV7. Two days after transfection, neurons were directly imaged every 10 s for a total of 161 images (30 min). (**A** and **B)** Quantification of the ratio of fission to fission plus events in axons (A) and dendrites (B) in live cultured neurons overexpressing TDP-43, while (**C)** is quantification in axons and dendrites in live cultured neurons knocking down TDP-43. Control: control neurons expressing mito-DsRed2 or mito-AcGFP only. Vector: vector neurons expressing empty vector; TDP-43 WT: neurons expressing wild-type TDP-43; TDP-43 Q331K: neurons expressing mutant TDP-43 Q331K; TDP-43 M337V: neurons expressing mutant TDP-43 M337V. Scrambled RNAi: neurons expressing scramble RNAi; TDP-43 RNAi: neurons expressing pre-miRNA to target TDP-43. At least 20 neurons were analyzed in each experiment and experiments were repeated three times. Data are means ± s.e.m. Statistics: one-way analysis of variance (ANOVA) followed by Tukey's multiple comparison test. $^{*}P < 0.05$, compared with control neuron.

and cell bodies of most motor neurons expressing both TDP-43 M337V and Mfn2 were comparable to that of control or vector control neurons, suggesting the complete prevention of TDP-43 induced mitochondria morphological abnormality. Strikingly, Mfn2 overexpression could even significantly increase mitochondrial length and density to the level comparable to control cells in TDP-43 M337V expressing neurons with abnormal cytoplasmic localization. We further measured the effect of Mfn2 overexpression on TDP-43 M337V induced mitochondrial transportation abnormalities in cultured neurons by live imaging. As shown in Supplementary Material, Figure S6, Mfn2 overexpression again could significantly improve mitochondrial movement in both axons and dendrites of neurons expressing TDP-43 M337V. The protective effect of Mfn2 on mitochondrial movements was again very effective in neurons with abnormal TDP-43 localization.

Mfn2 overexpression prevents TDP-43 induced mitochondrial dysfunction

Mitochondrial function is affected by changes in mitochondrial morphology (20). To assess the effect of TDP-43 overexpression on mitochondrial function, motor neurons were transfected with BFP tagged TDP-43 at DIV 7. Two days after transfection, mitochondrial reactive oxygen species (ROS) and mitochondria membrane potential (MMP) were measured as described previously (20). Compared with control or vector cells, mitochondrial ROS levels measured by mitoSOX were significantly elevated in neurons overexpressing mutant TDP-43 M337V while mitochondrial membrane potential measured by TMRM were significantly reduced (Fig. 10A and B). Interestingly, neurons with abnormal TDP-43 localization demonstrated more elevated ROS and lower MMP compared with those neurons with normal nuclear localization of TDP-43. To explore whether there is a causal relationship between mitochondrial dynamic abnormalities and dysfunction in neurons overexpressing TDP-43 M337V, we next measured mitochondrial ROS and MMP in neurons with Mfn2 overexpression. Interestingly, along with the prevention of mitochondrial dynamics abnormalities, the overproduction of mitochondrial ROS and the reduction in MMP caused by TDP-43 M337V overexpression could almost be completely prevented by Mfn2 overexpression even in neurons with abnormal TDP-43 localization. These results indicate that TDP-43-induced mitochondria dysfunction was secondary to mitochondrial dynamic abnormalities.

DISCUSSION

Many pathogenic mutations of TDP-43 have been found in both familial and common sporadic forms of ALS (21). As mitochondrial dysfunction represents a critical event in the pathogenesis of ALS and mitochondrial dysfunction is highly dependent on mitochondrial dynamics, we investigated the effect of ALS-associated mutant on mitochondrial dynamics and mitochondrial function in primary motor neurons. We first demonstrated that overexpression of mutant but not WT TDP-43 tipped the mitochondrial fission and fusion balance towards fission and caused mitochondrial fragmentation in dendrites and cell bodies, i.e. somatodendrites, rather than axons of motor neurons, whereas TDP-43 knockdown tipped the balance towards fusion and led to mitochondrial elongation. Either overexpression or knockdown of TDP-43 had been reported to affect neuronal viability by other groups (22–24). Thus, the mitochondrial morphological change we observed was unlikely the side effect of TDP-43 manipulation and should be the specific function of TDP-43 on mitochondria. We also demonstrated that mitochondrial density in dendrites but not axons was significantly reduced by WT TDP-43 overexpression and further reduced by ALS-associated mutant. In addition to the change of mitochondrial morphology, consistent with previous findings (13,14), we also observed aggregation of

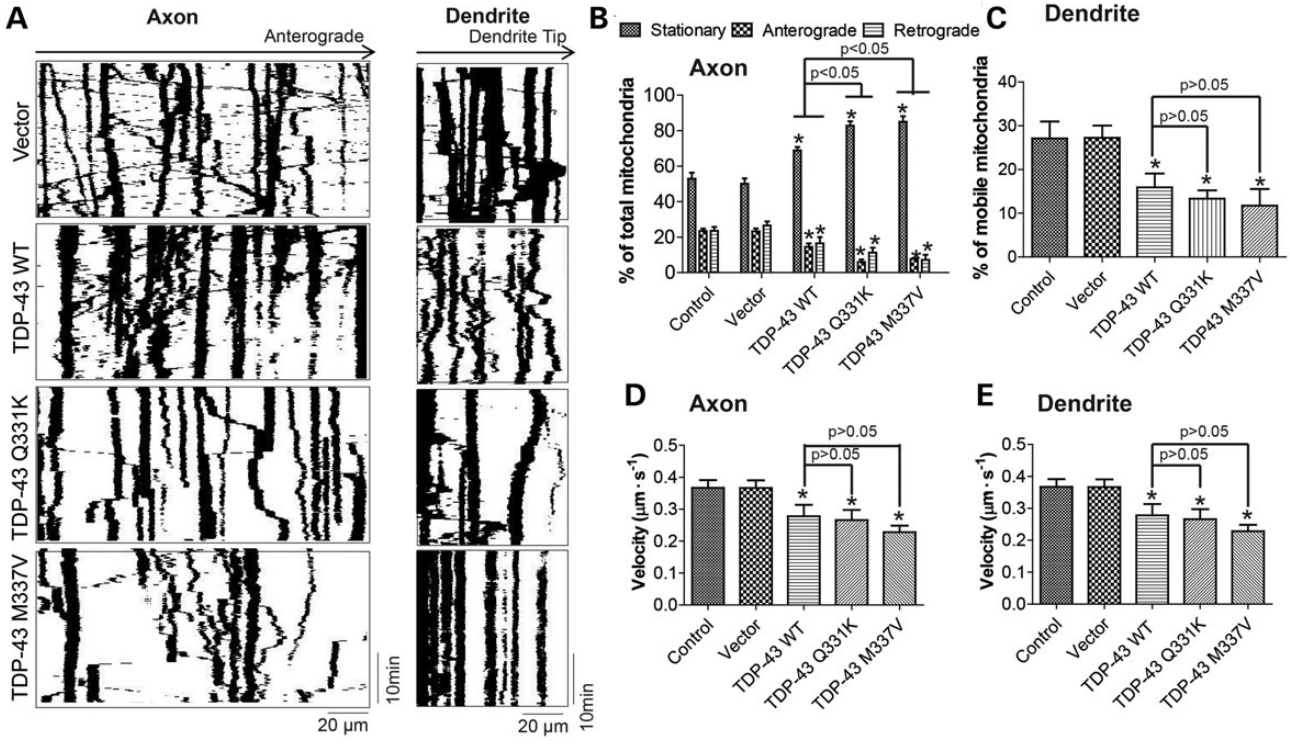

Figure 5. Effect of TDP-43 overexpression on mitochondrial movement in axon and dendrite. (**A**) Representative kymographs showing transport of mitochondria in live cultured primary rat motor neurons at DIV9 co-transfected with constructs encoding BFP tagged TDP-43 and mito-DsRed2 at DIV7. Neurons were directly imaged every 10 s for a total of 161 images (30 min). Vector: vector neurons expressing empty vector; TDP-43 WT: neurons expressing wild-type TDP-43; TDP-43 Q331K: neurons expressing mutant TDP-43 Q331K; TDP-43 M337V: neurons expressing mutant TDP-43 M337V. Left panels: kymographs showing transport of mitochondria in axons; Right panels: kymographs showing transport of mitochondria in dendrites. (**B** and **C**) Quantification of the proportion of non-mobile mitochondria and mitochondria moving in anterograde and retrograde directions in axons (B) and the proportion of mobile mitochondria in dendrites (C). (**D** and **E**) Quantification of the average velocity of mobile mitochondria in axons (D) and dendrites (E). Control: control neurons expressing mito-DsRed2 only. At least 20 neurons were analyzed in each experiment and experiments were repeated three times. Data are means ± s.e.m. Statistics: one-way analysis of variance (ANOVA) followed by Tukey's multiple comparison test. $^{*}P < 0.05$, compared with control neuron.

mitochondria in cells bodies of some neurons overexpressing TDP-43.

TDP-43 outside of nucleus mainly resides in the somatodendrites (25). As TDP-43 mainly affected mitochondria morphology and distribution/density in somatodendrites, our data indicated that TDP-43 might directly regulate local mitochondrial dynamics in somatodendrites rather than indirectly affect mitochondrial dynamics through nuclear gene expression regulation. To further support this notion, we provided evidence demonstrating the colocalization of TDP-43 and mitochondria in dendrites of primary motor neurons and the presence of TDP-43 in the purified mitochondrial fraction prepared from NSC34 motor neuronal cells. The TDP-43 localization on mitochondria was significantly enhanced by ALS-associated mutant TDP-43 Q331K and M337V. As ALS mutants caused more severe mitochondrial morphological changes, our data suggested that mitochondria might be a possible site of action for TDP-43 and mutant TDP-43 induced more severe mitochondrial dynamic abnormalities through enhanced association with mitochondria. mRNAs are present in dendritic processes and the local translation of dendritic mRNAs contributes to synaptic plasticity (26). It is also possible that TDP-43 affects mitochondrial dynamics by regulation of the local gene expression or RNA processing. Along this line, it will be interesting to see whether mitochondrial DNA transcription or mitochondrial RNA processing could also be affected by TDP-43 expression. In our experimental system, we did not see the significant change of mitochondria in axons of neurons overexpressing TDP-43. A potential explanation could be due to the relatively low level of TDP-43 in axons that does not reach a threshold to initiate mitochondrial morphological alterations.

Both WT and mutant TDP-43 overexpression significantly impaired mitochondrial movement in both dendrites and axons, and ALS-associated mutants further exacerbated its toxic action on mitochondrial movement in axons but not dendrites. TDP-43 could be transported in axons and regulate axon outgrowth (18). And the most recent study showed that the local mRNA translation in axons regulated mitochondrial function, axonal transportation and axonal maintenance (27). Thus, it is also possible that TDP-43 affects mitochondrial transportation through mediating local axonal mRNAs processing or translation. TDP-43 colocalized with mitochondria in axons of motor neurons and their colocalization was increased by ALS mutants, suggesting that the mitochondrial association of TDP-43 might again underlie TDP-43 induced mitochondrial transport impairment. We did not see significant difference between WT and mutant TDP-43 on mitochondrial movement in dendrites, perhaps due to the relative high level of TDP-43

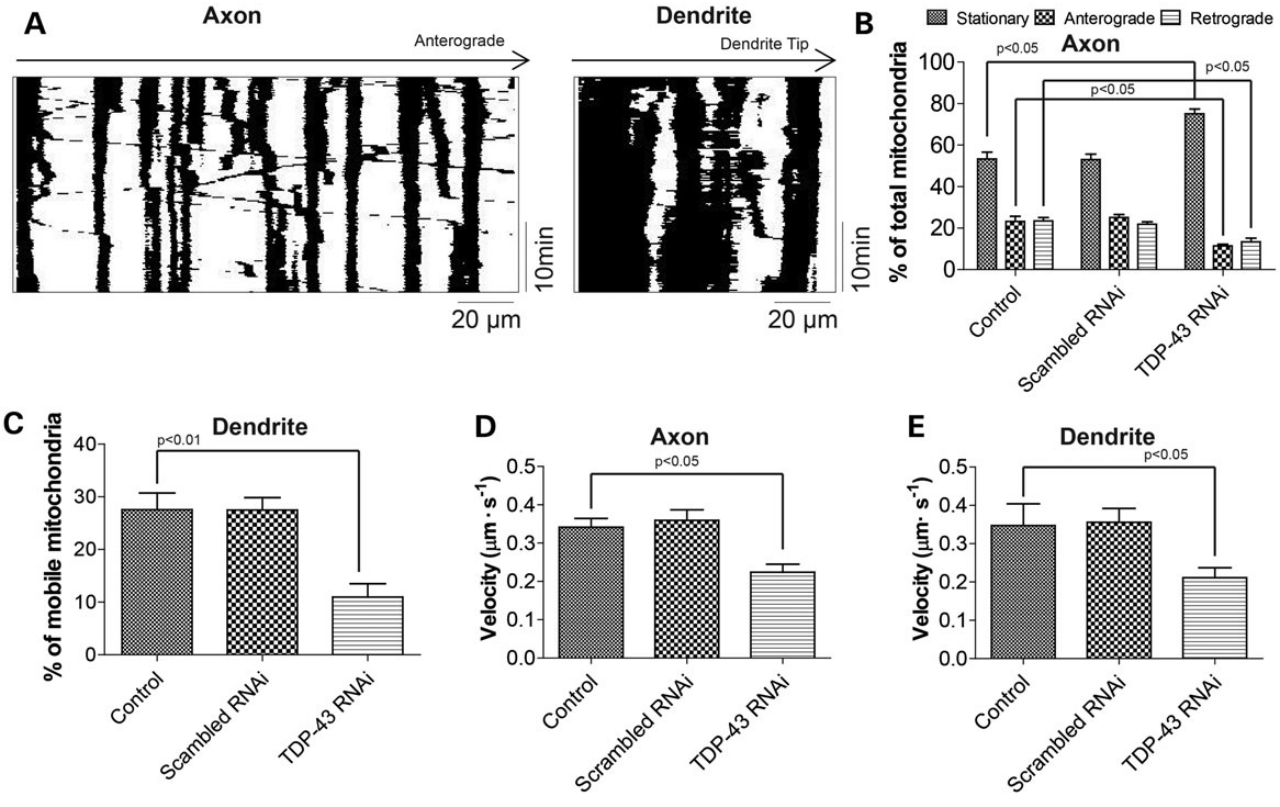

Figure 6. Effect of TDP-43 knockdown on mitochondrial movement in axon and dendrite. (**A**) Representative kymographs showing transport of mitochondria in live cultured primary rat motor neurons at DIV9 co-transfected with constructs encoding DsRed tagged TDP-43 RNAi and mito-AcGFP at DIV7. Neurons were directly imaged every 10 s for a total of 161 images (30 min). Left panel: kymograph showing transport of mitochondria in axons. Right panel: kymograph showing transport of mitochondria in dendrites. (**B** and **C**) Quantification of the proportion of non-mobile mitochondria and mitochondria moving in anterograde and retrograde directions in axons (B) and the proportion of mobile mitochondria in dendrites (C). (**D** and **E**) Quantification of the average velocity of mobile mitochondria in axons (D) and dendrites (E). Control: control neurons expressing mito-DsRed2 only. Scrambled RNAi: neurons expressing scramble RNAi; TDP-43 RNAi: neurons expressing pre-miRNA to target TDP-43. At least 20 neurons were analyzed in each experiment and experiments were repeated three times. Data are means ± s.e.m. Statistics: one-way analysis of variance (ANOVA) followed by Tukey's multiple comparison test.

in dendrites that saturates the effect of TDP-43 on mitochondria movement. As we did not see any mitochondrial morphology change in axon, it is unlikely that TDP-43 regulates mitochondrial movement directly through its effect on mitochondrial fission and fusion dynamics. The mechanism and relevance of the mitochondrial localization of TDP-43 in axons is still not clear. It will be interesting to assess whether TDP-43 affects local translation of proteins regulating mitochondrial movement such as kinesin and dynein (28). We also measured mitochondrial movement in motor neurons knocking down TDP-43. Surprisingly, TDP-43 knockdown also impaired rather than enhanced mitochondrial movement in both dendrites and axons. TDP-43 expression is tightly autoregulated (29) and the overexpression of exogenous TDP-43 was reported to suppress endogenous TDP-43 expression (24). In this scenario, it is possible that overexpression of mutant TDP-43 impairs mitochondria movement through the inhibition of normal TDP-43 function. One explanation for overexpression of WT TDP-43 also causing mitochondrial movement deficits could be that TDP-43 regulates multiple target genes that are involved in mitochondrial movement and TDP-43 overexpression and reduction/dysfunction affects mitochondrial movement through different pathways.

Cytoplasmic deposition of TDP43 was reported in ALS patients and animal models (2,13,14). Abnormal cytoplasmic TDP43 localization was also observed in TDP43 overexpressing cells in previous studies from multiple groups (18,23,30) and this study. It is a fundamental question to be answered what causes cytosolic localization of TDP43 and possible causes of abnormal localization, either due to general impact of overexpression or mutation effect on the health of cells, should not be ruled out. We reported here that abnormal cytoplasmic localization of TDP43 was associated with more severe mitochondrial dynamic abnormalities. Abnormal cytoplasmic TDP43 localization may be a consequence of perturbed cell health as reflected by severe mitochondrial dynamic abnormalities. In other words, abnormal TDP43 localization may be a consequence rather than the cause of abnormal mitochondrial dynamics. However, after further experimentation, we found that Mfn2 overexpression had no effect on the frequency of cytoplasmic TDP43 localization. As Mfn2 overexpression improves mitochondrial function and also likely improves cell health, this finding suggests that the abnormal TDP43 localization is unlikely a non-specific consequence of perturbed cell health at least using mitochondrial function as a parameter for cell health. It still could not be completely ruled out that other aspects of cell health may be impaired by

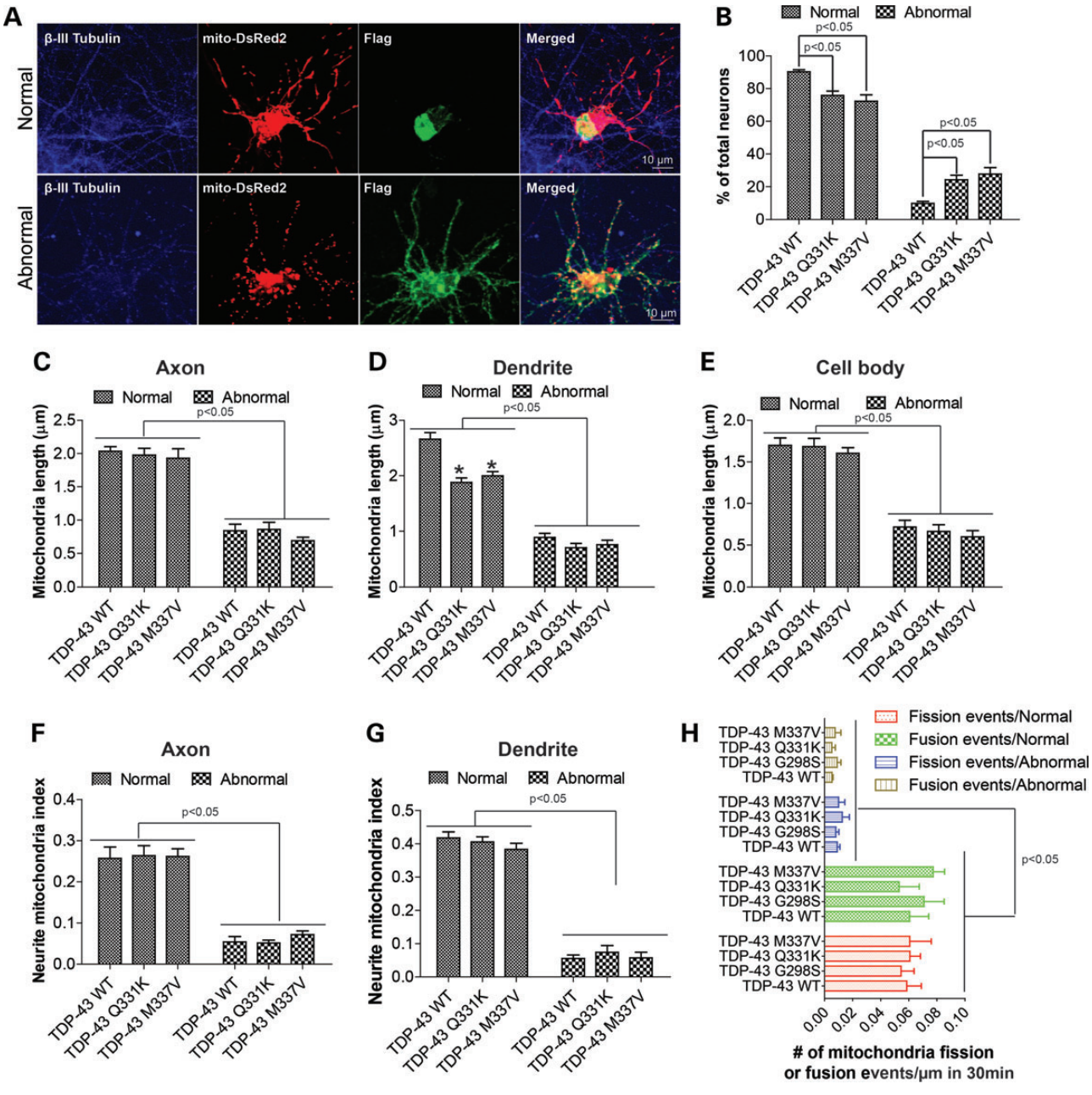

Figure 7. Mitochondrial morphological dynamics in motor neurons with abnormal cytoplasmic exogenous TDP-43. Primary rat motor neurons were co-transfected with flag/BFP tagged TDP-43 and mito-DsRed2/mito-AcGFP at DIV7, fixed at DIV9 and stained with antibodies against pan neuronal marker β-III tubulin and flag. (**A**) Representative confocal images of mitochondria in motor neurons expressing flag tagged WT TDP-43 and showing either normal nuclear and abnormal cytoplasmic localization of exogenous TDP-43. Blue: β-III tubulin; Green: flag; Red: mito-DsRed2. (**B**) Quantification of the percentage of neurons showing normal or abnormal exogenous TDP-43. (**C**–**E**) Quantification of mitochondrial length in axons (C), dendrites (D) and cell bodies (E). (**F** and **G**) Quantification of mitochondrial density (neurite mitochondrial index) in axons (F) and dendrites (G). (**H**) Quantification of the number of fission and fusion event in axons of neurons overexpressing BFP-tagged TDP43 and mito-DsRed2 at DIV9. Images were captured every 10 s for a total of 161 images (30 min). At least 30 neurons were analyzed in each experiment and experiments were repeated three times. Data are means ± s.e.m. Statistics: one-way analysis of variance (ANOVA) followed by Tukey's multiple comparison test. $^{*}P < 0.05$, compared with neuron expressing WT TDP-43.

TDP43 overexpression or mutation that may cause abnormal TDP43 localization. Nevertheless, our study likely places abnormal mitochondrial dynamics, our main observation in this study, downstream of abnormal TDP43 localization. It remains to be determined whether abnormal TDP43 localization is directly involved in the regulation of mitochondrial dynamics and whether other more fundamental root causes are involved which will be pursued in future studies.

There is still a great deal of debate about whether TDP-43 cytoplasmic accumulation or nuclear depletion is the potential pathogenic mechanism leading to TDP-43 dysfunction.

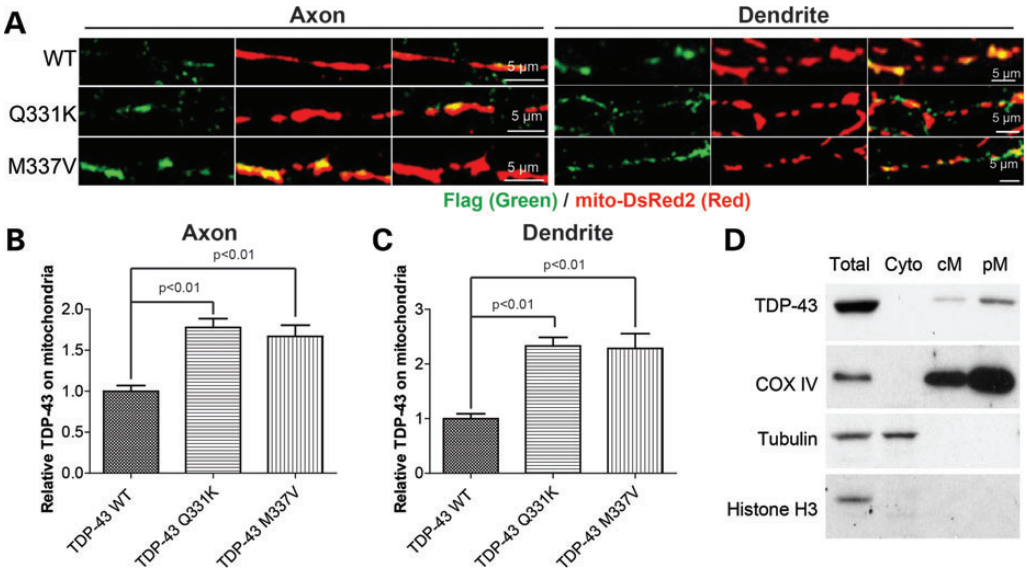

Figure 8. Co-localization of TDP-43 and mitochondria in motor neurons. Primary rat motor neurons were co-transfected with flag tagged TDP-43 and mito-DsRed2 at DIV7, fixed at DIV9 and stained with antibodies against flag. (**A**) Representative confocal images showing the colocalization of TDP-43 and mitochondria in axons and dendrites of neurons expressing flag tagged WT or mutant TDP-43. (**B** and **C**) Quantification of the relative TDP-43 localized on mitochondria (relative ratio of the intensity of TDP-43 green signal to the intensity of mito-DsRed2) in motor neurons expressing flag tagged WT or mutant TDP-43. (**D**) Representative immunoblot analysis of subcellular cellular fractionation shows the presence of TDP-43 in the highly purified mitochondria. Total: total cell lysate; Cyto: Cytosolic fraction; cM: crude mitochondria; pM, purified mitochondria. COXIV: mitochondrial marker; Tubulin: cytosol marker; Histone H3: nuclear marker. At least 10 neurons were analyzed in each experiment and experiments were repeated three times. Data are means ± s.e.m. Statistics: one-way analysis of variance (ANOVA) followed by Tukey's multiple comparison test.

Based on the observation that TDP43 knockdown, which depletes TDP43 from nucleus causes mitochondrial elongation while overexpression of TDP43 mutants that leads to abnormal cytoplasmic accumulation and nuclear depletion of TDP43 (i.e. abnormal TDP43 localization) causes mitochondrial fragmentation, we concluded that it is the cytoplasmic accumulation rather than nuclear depletion that mediates the toxic effect of TDP43 mutants on mitochondrial abnormalities (i.e. fragmentation and dysfunction). Nevertheless, it remains to be determined what causes cytosolic deposition and nuclear depletion of TDP43 in TDP43 overexpressing cells and, it cannot be completely ruled out that the abnormal localization could be due to general impact of overexpression or mutation on the health of cells.

In those neurons with abnormal TDP-43 localization, we did not observe any significant difference of mitochondrial dynamics between WT and mutant TDP-43, suggesting that machineries regulating mitochondrial dynamics are probably severely damaged and mask the possible difference between WT and mutant TDP-43. And, it should be emphasized that all neurons with abnormal TDP-43 localization exhibited severe perinuclear aggregation of mitochondria in cell bodies and were devoid of mitochondria in neurites. Neurons are particularly sensitive to perturbations in mitochondrial distribution (31) and proper density and localization of mitochondria is of critical importance for the maintenance of synapses (32–34). In ALS patients, synaptic loss occurs long before neuronal loss (35). As the cytoplasmic TDP-43 localization was a prevalent and early feature in most affected sporadic ALS neurons (36), our data suggested that TDP-43-induced abnormal mitochondrial distribution likely underlies the synaptic loss in ALS neurons bearing TDP-43 mutant. It may also play such a role in sporadic ALS neurons with TDP-43 proteinopathy.

Mfn2 regulates both mitochondrial morphology and movement. It was not surprising to see that Mfn2 overexpression substantially alleviated TDP-43-induced mitochondrial morphological and movement abnormalities in motor neurons. The protective effect of Mfn2 indeed further suggested the specific role of TDP-43 in regulating mitochondrial dynamics. Mitochondria fission and fusion dynamics are tightly regulated by mitochondrial fission and fusion proteins, i.e. DLP1 and its recruiting factors on mitochondria such as Fis1, Mff, MiD49 and MiD51 for fission (37) and Mfn1, Mfn2 and OPA1 for fusion (10). Previous studies demonstrated that TDP-43 overexpression changed the protein levels of DLP1, Mfn1 and Fis1. Unfortunately, the levels of Mfn2 and other mitochondrial fission and fusion proteins were not measured. It is possible that TDP-43 regulates the expression of multiple mitochondrial fission and fusion proteins. Further experiments will be necessary to measure the effect of TDP-43 manipulation on all mitochondrial fission and fusion proteins as well as other proteins involved in mitochondrial movement. Mutant TDP-43 induced mitochondrial dysfunction, which correlated well with mitochondrial dynamic abnormalities. And, more importantly, mutant TDP-43 induced mitochondrial dysfunction could be substantially ameliorated by Mfn2, suggesting a specific role of mitochondrial dynamics in mediating the toxicity of TDP-43 on mitochondria function.

Together, our study provides a detailed understanding of ALS-associated TDP-43 mutant in the regulation of mitochondrial dynamics and function, and suggests mitochondrial dynamics as potential new targets for therapeutic intervention in ALS.

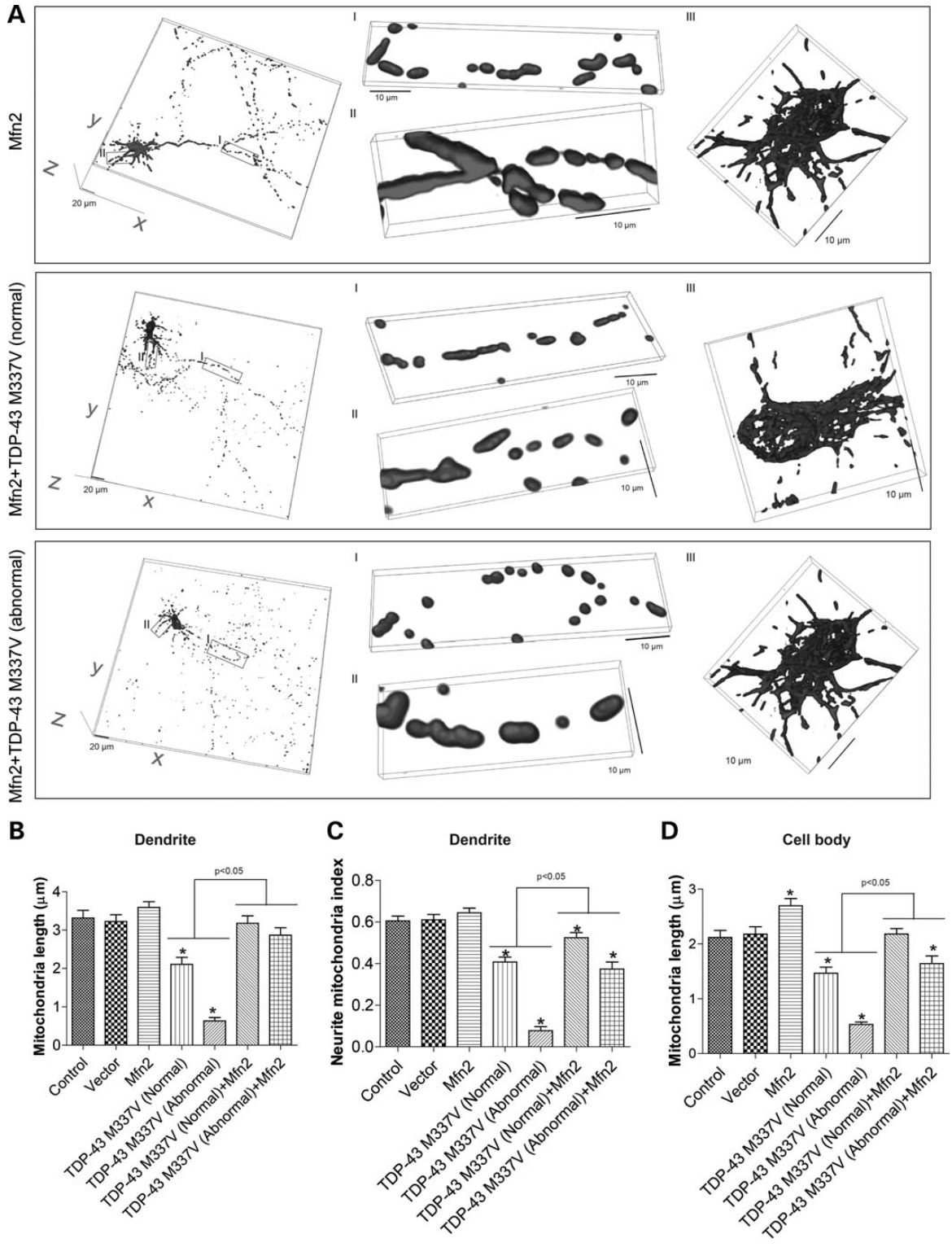

Figure 9. Rescue of mutant TDP-43 induced mitochondrial fragmentation by Mfn2 overexpression. (**A**) Representative 3D pictures of mitochondria in primary rat motor neurons at days *in vitro* 9 (DIV9) co-transfected with constructs encoding BFP tagged TDP-43 M337V, GFP tagged Mfn2 and mito-DsRed2 at DIV7. Mfn2: neurons overexpressing Mfn2 only; Mfn2+TDP-43 WT (normal): neurons overexpressing both Mfn2 and mutant TDP-43 M337V and showing normal nuclear localization of TDP-43; Mfn2 + TDP-43 WT (abnormal): neurons overexpressing both Mfn2 and mutant TDP-43 M337V and showing abnormal cytoplasmic localization of TDP-43. Left panels: large field of view of mitochondria in motor neurons. Middle panels: enlargement showing mitochondria in axons (enlargement I) and dendrites (enlargement II). Right panels: enlargement showing mitochondria in cell bodies (enlargement III). (**B**–**D**) Quantification of mitochondria length (B) and density (i.e. neurite mitochondria index) (C) in dendrites. (D) Quantification of mitochondria length in cell bodies. Control: control neurons expressing mito-DsRed2 only. At least 20 neurons were analyzed in each experiment and experiments were repeated 3 times. Data are means $\pm$ s.e.m. Statistics: one-way analysis of variance (ANOVA) followed by Tukey's multiple comparison test. $^{*}P < 0.05$, compared with control neuron.

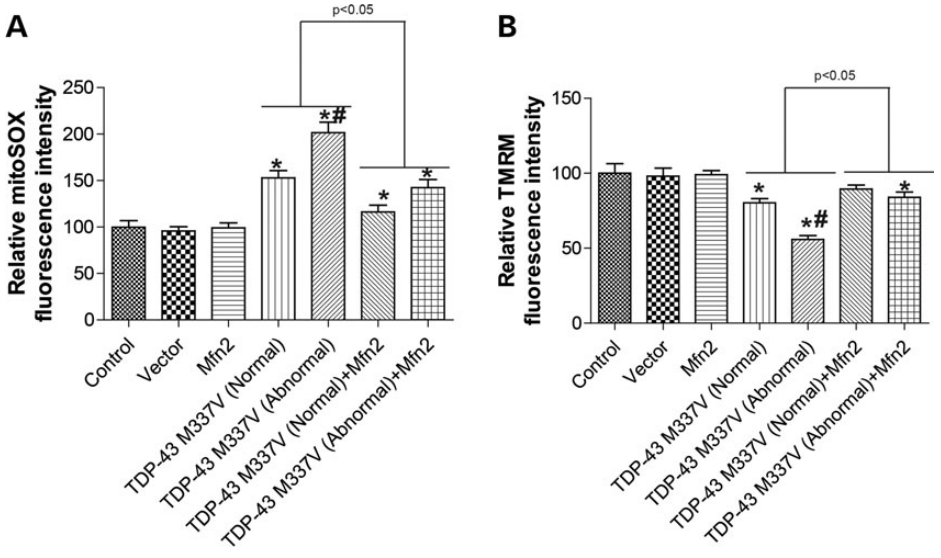

Figure 10. Rescue of mutant TDP-43 induced mitochondrial dysfunction by Mfn2 overexpression. Motor neurons were seeded on 24-well plates and transfected with GFP tagged Mfn2 or BFP tagged mutant TDP-43 or co-transfected with GFP tagged Mfn2 and BFP tagged mutant TDP-43 at DIV7. At DIV9, the mitochondrial ROS and mitochondrial membrane potential (MMP) were measured by mitoSOX and TMRM respectively. (**A** and **B**) Quantification of the relative fluorescent intensity of mitoSOX (A) and TMRM (B) in cell bodies of motor neurons. At least 50 neurons were analyzed in each experiment and experiments were repeated three times. Data are means ± s.e.m. Statistics: one-way analysis of variance (ANOVA) followed by Tukey's multiple comparison test. $^{*}P < 0.05$, compared with control neuron and $^{\#}P < 0.05$, compared with neurons expressing TDP-43 M337V with normal TDP-43 localization.

MATERIALS AND METHODS

Embryonic primary motor neuron isolation, cell culture and cell transfection

Timed pregnant Harlan–Sprague–Dawley rats were sacrificed following the protocol approved by the Institutional Animal Care and Use Committee (IACUC) at Case Western Reserve University. E13–15 rat embryos were obtained and primary motor neurons were isolated generally as described before (38,39) but with some modifications. Taken briefly, the spinal cords were dissected out in L15 medium without phenol red (Invitrogen) and stored in Hibernate E (BrainBits) supplemented with 2% B27 (Invitrogen). Under a dissecting microscope, dorsal root ganglia were carefully removed from the spinal cords and the meninges were removed completely with fine forceps. Whole spinal cords were then digested in 0.25% trypsin for 15 min at room temperature followed by brief incubation in Opti-MEM (Invitrogen) supplemented with 10% FBS and 50 units/ml DNAse I (Worthington-biochem). Spinal cords were dissociated by gentle trituration with pipette until the cell suspension was homogenous and no large pieces of tissue remain visible. Motor neurons were then purified in 6% Optiprep (Sigma) in L15 medium without phenol red (Invitrogen) by gradient centrifugation. Glia cells in the bottom layer were obtained first, grown on six-well plates in MEM medium (Invitrogen) supplement with 10% FBS and 1% penicillin–streptomycin for 4 h and then incubated with Neurobasal medium (Invitrogen) supplemented with 2% B27 (Invitrogen) and 1% GlutaMax (Invitrogen) for 24 h to obtain glia-conditioned media. Motor neurons in the top layer were collected and seeded on poly-L-lysine/laminin-coated coverslips/chamber slides (BD), 35 mm dishes or 24-well plates in Neurobasal medium (Invitrogen) supplemented with 2% B27 (Invitrogen), 1% GlutaMax (Invitrogen) and 1% penicillin–streptomycin. Four hours after seeding, motor neurons were switched to glia-conditioned medium supplemented with 2% horse serum (Sigma), and 10 ng/ml each BDNF, CNTF and GDNF (Peprotech) (38). Half the culture medium was changed every 3 days. All cultures were kept at 37°C in a humidified 5% CO_2 containing atmosphere. Most of the cells were neurons after they were cultured for 9 days of culture *in vitro* (DIV), which was verified by positive staining for the pan neuronal marker β-III tubulin and motor neuron specific markers Islet-1 and Hb9. At DIV7, neurons were transfected using NeuroMag transfection reagent (Oz Biosciences) according to manufacturer's protocol. For co-transfection, a 3:1 or 3:1:1 ratio (TDP-43: mito-DsRed2 or TDP-43:Mfn2: mito-DsRed2) was applied. Mouse motor neuron-like hybrid cells (NSC-34, gift of Dr Neil Cashman, University of Toronto) were grown in DMEM without sodium pyruvate (Sigma), supplemented with 10% (v/v) fetal bovine serum (Invitrogen) and 1% penicillin–streptomycin (Invitrogen), in 5% CO2 in a humid incubator at 37°C.

Expression vectors, antibodies, chemicals and measurements

Mito-DsRed2 (Clontech), GFP-tagged Mfn2 (gift of Dr Margaret T. Fuller, Stanford University), tdTomato tagged wild-type human TDP-43 (wtTDP43tdTOMATOHA, Addgene) and DsRed-tagged microRNA expression construct miR-TDP-43b (miR-TDP43b, Addgene) were obtained. Mito-AcGFP was described before (20). Blue fluorescent protein (BFP) tagged TDP-43 were generated by replacing tdTomato in wtTDP43tdTOMATOHA by PCR-based In-Fusion® HD Cloning Kit (Clontech). The expression plasmid for flag-tagged TDP-43 was constructed based on the pCMV-3Tag-1 Vector (Agilent). TDP-43 Q331K and M337V mutants were generated through site-directed mutagenesis by using QuikChange Lightning Site-Directed Mutagenesis

Kits (Agilent). Primary antibodies used included rabbit anti-flag/COV IV (Cell Signaling), mouse anti-flag (Sigma), mouse anti-β-III tubulin (Cell Signaling), rabbit anti-HB9/Islet-1 (Millipore), rabbit anti-TDP-43/Histone H3 (Cell Signaling), rabbit anti-α-tubulin (Epitomics) and chemicals (Sigma) were obtained. The mitochondrial ROS level and mitochondrial membrane potential was measured as described before using mitoSOX and TMRM (Invitrogen), respectively (20).

Mitochondria isolation and western blot analysis

Crude and purified mitochondria was isolated as described before (40) with some modifications. Briefly, cells were trypsinized, washed in PBS and suspended in a minimal volume of IB-1 solution (IB-1: 225 mM Manitol, 75 mM sucrose, 0.1 mM EGTA, 20 mM HEPES; pH = 7.4). The cells were homogenized and centrifuged at 600*g* at 4°C for 5 min for two times to remove nuclear contaminants and unbroken cells. The supernatant was then centrifuged at 7000*g* at 4°C for 10 min to obtain enriched mitochondria fraction and the supernatant was collected as the cytosolic fraction. The enriched mitochondrial fraction was further centrifuged at 7000*g* at 4°C for 10 min, suspended in IB-2 solution (225 mM Manitol, 75 mM sucrose, 20 mM HEPES; pH = 7.4), centrifuged at 10 000*g* for 10 min and finally suspended in MRB buffer (250 mM Manitol, 0.5 mM EGTA, 5 mM HEPES; pH 7.4) to obtain crude mitochondrial fraction. The crude mitochondrial fraction was overlaid on top of 8 ml Percoll medium [225 mM manitol, 25 mM HEPES, 1 mM EGTA and 30% Percoll (vol/vol); pH = 7.4] and was subjected to centrifugation at 95 000*g* for 30 min at 4°C in a Beckman SW40 Ti rotor. The pellet was suspended in MRB buffer followed by centrifugation at 6300*g* for 10 min at 4°C to obtained purified mitochondria. Purified mitochondria or cells were lysed with ×1 Cell Lysis Buffer (Cell Signaling) plus 1 mM PMSF (Sigma) and Protease Inhibitor Cocktail (Sigma). Equal amounts of total protein extract (10 μg) were resolved by SDS–PAGE and transferred to Immobilon-P (Millipore). Following blocking with 10% non-fat dry milk, primary and secondary antibodies were applied as previously described (41) and the blots developed with Immobilon Western Chemiluminescent HRP Substrate (Millipore).

Immunofluorescence, time-lapse imaging and electron microscopy

For immunofluorescence, neurons cultured on coverslips or chamber slides were fixed and stained as described previously (41). All fluorescence images of fixed were captured at room temperature with a Zeiss LSM 510 inverted laser-scanning confocal fluorescence microscope (controlled through Zeiss LSM 510 confocal software, Zeiss) equipped with a C-Apochromat 40X/1.2W water objective or alpha Plan-Fluar ×100/1.45 oil objective as previously described (42). Confocal images of far-red fluorescence were collected using 633 nm excitation light from a HeNe laser and a 650 nm long-pass filter; images of red fluorescence were collected using 543 nm excitation light from an argon laser and a 560 nm long-pass filter; and green fluorescence images were collected using 488 nm excitation light from an argon laser and a 500–550 nm bandpass barrier filter. For time-lapse imaging, neurons were seeded in 35 mM dishes and transfected with mito-DsRed2/mito-AcGFP. 48 h after transfection, neurons were placed in a well-equipped environmental chamber with controlled CO_2 content, humidity and temperature and imaged at 37°C by an inverted Leica DMI6000 fluorescence microscope (Leica) (controlled through Leica LAS AF 3 software) with a 20X/0.7NA Plan Apochromat dry objective. During time-lapse imaging, frames were captured every 5 or 10 s for at least 1 h without phototoxicity or photobleaching.

One-month-old non-transgenic mice (NTG) and transgenic mice overexpressing WT or M337 V mutant TDP-43 under the control of the mouse PRNP (prion protein) promoter (i.e. WT and M337 V mice) were perfused with 4%-paraformaldehyde (pFA) or 2.5% glutaraldehyde (GA)-2% pFA in 0.1 M cacodylate buffer. Spinal cords were removed and further fixed in 2.5% GA-2% pFA, post-fixed in 1% OsO_4, dehydrated in alcohols and propylene oxide, infiltrated and embedded in Epon 812. Ultrathin sections mounted on copper grids were stained with uranyl acetate and lead citrate, and examined in an electron microscope Philips 208S electron microscope with a Gatan CCD camera.

Image analysis

Image analysis was also performed with open-source image-analysis programs WCIF ImageJ (developed by W. Rasband). Mitochondria morphology was quantified as previously described (43). Taken briefly, single plane or series of z-stacks of raw images were background corrected, linearly contrast optimized, applied with a 7 × 7 'top hat' filter, subjected to a 3 × 3 median filter and then thresholded to generate binary images. Most mitochondria were well separated in binary images and large clusters of mitochondria were excluded automatically. All binary images were either directly analyzed or assembled into 3D volumes by Image J.

SUPPLEMENTARY MATERIAL

Supplementary Material is available at *HMG* online.

Conflict of Interest statement. None declared.

FUNDING

This study is supported by grants from National Institutes of Health (R03AG044680 to X.W.), Advanced Studies and Visiting Program for Young College Teachers at Shanghai Municipal Education Commission (to L.L.) and the Program for Professor of Special Appointment (Eastern Scholar) at Shanghai Municipal Education Commission and Key Disciplines of Clinical Integrative Chinese and Western Medicine at State Administration of Traditional Chinese Medicine of the People's Republic of China (to T.Z.)

REFERENCES

1. Cohen, T.J., Lee, V.M. and Trojanowski, J.Q (2011) TDP-43 functions and pathogenic mechanisms implicated in TDP-43 proteinopathies. *Trends Mol. Med.*, **17**, 659–667.

2. Neumann, M., Sampathu, D.M., Kwong, L.K., Truax, A.C., Micsenyi, M.C., Chou, T.T., Bruce, J., Schuck, T., Grossman, M., Clark, C.M. *et al.* (2006) Ubiquitinated TDP-43 in frontotemporal lobar degeneration and amyotrophic lateral sclerosis. *Science*, **314**, 130–133.
3. Amador-Ortiz, C., Lin, W.L., Ahmed, Z., Personett, D., Davies, P., Duara, R., Graff-Radford, N.R., Hutton, M.L. and Dickson, D.W. (2007) TDP-43 immunoreactivity in hippocampal sclerosis and Alzheimer's disease. *Ann. Neurol.*, **61**, 435–445.
4. Chanson, J.B., Echaniz-Laguna, A., Vogel, T., Mohr, M., Benoilid, A., Kaltenbach, G. and Kiesmann, M. (2010) TDP43-positive intraneuronal inclusions in a patient with motor neuron disease and Parkinson's disease. *Neurodegener. Dis.*, **7**, 260–264.
5. Davidson, Y., Amin, H., Kelley, T., Shi, J., Tian, J., Kumaran, R., Lashley, T., Lees, A.J., DuPlessis, D., Neary, D. *et al.* (2009) TDP-43 in ubiquitinated inclusions in the inferior olives in frontotemporal lobar degeneration and in other neurodegenerative diseases: a degenerative process distinct from normal ageing. *Acta Neuropathol.*, **118**, 359–369.
6. Buratti, E., Dork, T., Zuccato, E., Pagani, F., Romano, M. and Baralle, F.E. (2001) Nuclear factor TDP-43 and SR proteins promote *in vitro* and *in vivo* CFTR exon 9 skipping. *EMBO J.*, **20**, 1774–1784.
7. Buratti, E. and Baralle, F.E. (2010) The multiple roles of TDP-43 in pre-mRNA processing and gene expression regulation. *RNA Biol.*, **7**, 420–429.
8. Ling, S.C., Albuquerque, C.P., Han, J.S., Lagier-Tourenne, C., Tokunaga, S., Zhou, H. and Cleveland, D.W. (2010) ALS-associated mutations in TDP-43 increase its stability and promote TDP-43 complexes with FUS/TLS. *Proc. Natl Acad. Sci. USA*, **107**, 13318–13323.
9. Cozzolino, M. and Carri, M.T. (2012) Mitochondrial dysfunction in ALS. *Prog. Neurobiol.*, **97**, 54–66.
10. Detmer, S.A. and Chan, D.C. (2007) Functions and dysfunctions of mitochondrial dynamics. *Nat. Rev. Mol. Cell Biol.*, **8**, 870–879.
11. Liu, W., Acin-Perez, R., Geghman, K.D., Manfredi, G., Lu, B. and Li, C. (2011) Pink1 regulates the oxidative phosphorylation machinery via mitochondrial fission. *Proc. Natl Acad. Sci. USA*, **108**, 12920–12924.
12. Shi, P., Gal, J., Kwinter, D.M., Liu, X. and Zhu, H. (2010) Mitochondrial dysfunction in amyotrophic lateral sclerosis. *Biochim. Biophys. Acta*, **1802**, 45–51.
13. Xu, Y.F., Gendron, T.F., Zhang, Y.J., Lin, W.L., D'Alton, S., Sheng, H., Casey, M.C., Tong, J., Knight, J., Yu, X. *et al.* (2010) Wild-type human TDP-43 expression causes TDP-43 phosphorylation, mitochondrial aggregation, motor deficits, and early mortality in transgenic mice. *J. Neurosci.*, **30**, 10851–10859.
14. Xu, Y.F., Zhang, Y.J., Lin, W.L., Cao, X., Stetler, C., Dickson, D.W., Lewis, J. and Petrucelli, L. (2011) Expression of mutant TDP-43 induces neuronal dysfunction in transgenic mice. *Mol. Neurodegener.*, **6**, 73.
15. Yang, C.X., Tan, W.J., Whittle, C., Qiu, L.H., Cao, L.C., Akbarian, S. and Xu, Z.S. (2010) The C-terminal TDP-43 fragments have a high aggregation propensity and harm neurons by a dominant-negative mechanism. *PLoS One*, **5**, e15878.
16. Sasaki, S. and Iwata, M. (1996) Impairment of fast axonal transport in the proximal axons of anterior horn neurons in amyotrophic lateral sclerosis. *Neurology*, **47**, 535–540.
17. Sheng, Z.H. and Cai, Q. (2012) Mitochondrial transport in neurons: impact on synaptic homeostasis and neurodegeneration. *Nat. Rev. Neurosci.*, **13**, 77–93.
18. Fallini, C., Bassell, G.J. and Rossoll, W. (2012) The ALS disease protein TDP-43 is actively transported in motor neuron axons and regulates axon outgrowth. *Hum. Mol. Genet.*, **21**, 3703–3718.
19. Chen, H., Detmer, S.A., Ewald, A.J., Griffin, E.E., Fraser, S.E. and Chan, D.C. (2003) Mitofusins Mfn1 and Mfn2 coordinately regulate mitochondrial fusion and are essential for embryonic development. *J. Cell Biol.*, **160**, 189–200.
20. Wang, X., Su, B., Siedlak, S.L., Moreira, P.I., Fujioka, H., Wang, Y., Casadesus, G. and Zhu, X. (2008) Amyloid-beta overproduction causes abnormal mitochondrial dynamics via differential modulation of mitochondrial fission/fusion proteins. *Proc. Natl Acad. Sci. USA*, **105**, 19318–19323.
21. Pesiridis, G.S., Lee, V.M. and Trojanowski, J.Q. (2009) Mutations in TDP-43 link glycine-rich domain functions to amyotrophic lateral sclerosis. *Hum. Mol. Genet.*, **18**, R156–R162.
22. Iguchi, Y., Katsuno, M., Niwa, J., Yamada, S., Sone, J., Waza, M., Adachi, H., Tanaka, F., Nagata, K., Arimura, N. *et al.* (2009) TDP-43 depletion induces neuronal cell damage through dysregulation of Rho family GTPases. *J. Biol. Chem.*, **284**, 22059–22066.
23. Barmada, S.J., Skibinski, G., Korb, E., Rao, E.J., Wu, J.Y. and Finkbeiner, S. (2010) Cytoplasmic mislocalization of TDP-43 is toxic to neurons and enhanced by a mutation associated with familial amyotrophic lateral sclerosis. *J. Neurosci.*, **30**, 639–649.
24. Igaz, L.M., Kwong, L.K., Lee, E.B., Chen-Plotkin, A., Swanson, E., Unger, T., Malunda, J., Xu, Y., Winton, M.J., Trojanowski, J.Q. *et al.* (2011) Dysregulation of the ALS-associated gene TDP-43 leads to neuronal death and degeneration in mice. *J. Clin. Invest.*, **121**, 726–738.
25. Wang, I.F., Wu, L.S., Chang, H.Y. and Shen, C.K. (2008) TDP-43, the signature protein of FTLD-U, is a neuronal activity-responsive factor. *J. Neurochem.*, **105**, 797–806.
26. Bramham, C.R. and Wells, D.G. (2007) Dendritic mRNA: transport, translation and function. *Nat. Rev. Neurosci.*, **8**, 776–789.
27. Yoon, B.C., Jung, H., Dwivedy, A., O'Hare, C.M., Zivraj, K.H. and Holt, C.E. (2012) Local translation of extranuclear lamin B promotes axon maintenance. *Cell*, **148**, 752–764.
28. Saxton, W.M. and Hollenbeck, P.J. (2012) The axonal transport of mitochondria. *J. Cell Sci.*, **125**, 2095–2104.
29. Avendano-Vazquez, S.E., Dhir, A., Bembich, S., Buratti, E., Proudfoot, N. and Baralle, F.E. (2012) Autoregulation of TDP-43 mRNA levels involves interplay between transcription, splicing, and alternative polyA site selection. *Genes Dev.*, **26**, 1679–1684.
30. Estes, P.S., Boehringer, A., Zwick, R., Tang, J.E., Grigsby, B. and Zarnescu, D.C. (2011) Wild-type and A315 T mutant TDP-43 exert differential neurotoxicity in a Drosophila model of ALS. *Hum. Mol. Genet.*, **20**, 2308–2321.
31. Kann, O. and Kovacs, R. (2007) Mitochondria and neuronal activity. *Am. J. Physiol. Cell Physiol.*, **292**, C641–C657.
32. Stowers, R.S., Megeath, L.J., Gorska-Andrzejak, J., Meinertzhagen, I.A. and Schwarz, T.L. (2002) Axonal transport of mitochondria to synapses depends on milton, a novel Drosophila protein. *Neuron*, **36**, 1063–1077.
33. Melov, S. (2004) Modeling mitochondrial function in aging neurons. *Trends Neurosci.*, **27**, 601–606.
34. Guo, X.F., Macleod, G.T., Wellington, A., Hu, F., Panchumarthi, S., Schoenfield, M., Marin, L., Charlton, M.P., Atwood, H.L. and Zinsmaier, K.E. (2005) The GTPase dMiro is required for axonal transport of mitochondria to Drosophila synapses. *Neuron*, **47**, 379–393.
35. Dadon-Nachum, M., Melamed, E. and Offen, D. (2011) The "dying-back" phenomenon of motor neurons in ALS. *J. Mol. Neurosci.*, **43**, 470–477.
36. Giordana, M.T., Piccinini, M., Grifoni, S., De Marco, G., Vercellino, M., Magistrello, M., Pellerino, A., Buccinna, B., Lupino, E. and Rinaudo, M.T. (2010) TDP-43 Redistribution is an early event in sporadic amyotrophic lateral sclerosis. *Brain Pathology*, **20**, 351–360.
37. Loson, O.C., Song, Z., Chen, H. and Chan, D.C. (2013) Fis1, Mff, MiD49 and MiD51 mediate Drp1 recruitment in mitochondrial fission. *Mol. Biol. Cell.*, **24**, 659–667.
38. Fallini, C., Bassell, G.J. and Rossoll, W. (2010) High-efficiency transfection of cultured primary motor neurons to study protein localization, trafficking, and function. *Mol. Neurodegener.*, **5**, 17.
39. Wiese, S., Herrmann, T., Drepper, C., Jablonka, S., Funk, N., Klausmeyer, A., Rogers, M.L., Rush, R. and Sendtner, M. (2010) Isolation and enrichment of embryonic mouse motoneurons from the lumbar spinal cord of individual mouse embryos. *Nat. Protoc.*, **5**, 31–38.
40. Wieckowski, M.R., Giorgi, C., Lebiedzinska, M., Duszynski, J. and Pinton, P. (2009) Isolation of mitochondria-associated membranes and mitochondria from animal tissues and cells. *Nat. Protoc.*, **4**, 1582–1590.
41. Wang, X., Su, B., Fujioka, H. and Zhu, X. (2008) Dynamin-like protein 1 reduction underlies mitochondrial morphology and distribution abnormalities in fibroblasts from sporadic Alzheimer's disease patients. *Am. J. Pathol.*, **173**, 470–482.
42. Wang, X., Su, B., Lee, H.G., Li, X., Perry, G., Smith, M.A. and Zhu, X. (2009) Impaired balance of mitochondrial fission and fusion in Alzheimer's disease. *J. Neurosci.*, **29**, 9090–9103.
43. Koopman, W.J., Distelmaier, F., Esseling, J.J., Smeitink, J.A. and Willems, P.H. (2008) Computer-assisted live cell analysis of mitochondrial membrane potential, morphology and calcium handling. *Methods*, **46**, 304–311.